Submarine Groundwater and River Discharges Affect Carbon Cycle in a Highly Urbanized and River-Dominated Coastal Area

Xuejing Wang[1], Yan Zhang[2]*, Chunmiao Zheng[1], Manhua Luo[2], Shengchao Yu[1,3], Meiqing Lu[1,3] and Hailong Li[1]*

[1] State Environmental Protection Key Laboratory of Integrated Surface Water-Groundwater Pollution Control, School of Environmental Science and Engineering, Southern University of Science and Technology, Shenzhen, China, [2] MOE Key Laboratory of Groundwater Circulation and Environment Evolution and School of Water Resources and Environment, China University of Geosciences (Beijing), Beijing, China, [3] Department of Earth Sciences, The University of Hong Kong, Hong Kong, Hong Kong SAR, China

Riverine carbon flux to the ocean has been considered in estimating coastal carbon budgets, but submarine groundwater discharge (SGD) has long been ignored. In this paper, the effects of both SGD and river discharges on the carbon cycle were investigated in the Guangdong-HongKong-Macao Greater Bay Area (GBA), a highly urbanized and river-dominated coastal area in China. SGD-derived nitrate (NO_3^-), dissolved organic carbon (DOC), and dissolved inorganic carbon (DIC) fluxes were estimated using a radium model to be $(0.73-16.4) \times 10^8$ g/d, $(0.60-9.94) \times 10^9$ g/d, and $(0.77-3.29) \times 10^{10}$ g/d, respectively. SGD-derived DOC and DIC fluxes are ~ 2 times as great as riverine inputs, but SGD-derived NO_3^- flux is one-fourth of the riverine input. The additional nitrate and carbon inputs can stimulate new primary production, enhance biological pump efficiency, and affect the balance of the carbonate system in marine water. We found that SGD in the studied system is a potential net source of atmospheric CO_2 with a flux of 1.46×10^9 g C/d, and river, however, is a potential net sink of atmospheric CO_2 with a flux of 3.75×10^9 g C/d during the dry winter season. Two conceptual models were proposed illustrating the major potential processes of the carbon cycle induced by SGD and river discharges. These findings from this study suggested that SGD, as important as rivers, plays a significant role in the carbon cycle and should be considered in carbon budget estimations at regional and global scales future.

Keywords: submarine groundwater discharge (SGD), river, radium isotopes, dissolved carbon, Greater Bay Area

INTRODUCTION

Nutrient budgets in the ocean are subject to a variety of influences such as surface rivers, submarine groundwater discharge (SGD), and the atmosphere. River is a visible pathway of biogenic substances such as nitrogen, phosphorus, and carbon from the land to the ocean, and plays a vital role in the global carbon and nitrogen cycles (Cole et al., 2007; Dai et al., 2012).

The global riverine carbon flux was estimated to be (1.9–2.7) $\times 10^{15}$ g/year, in which the organic component accounts for approximately 45% (Cole et al., 2007; Cai, 2011). As the largest river in the Guangdong-HongKong-Macao Greater Bay Area (GBA), the Pearl River delivers about 1.27×10^{13} g/year of carbon to the estuary and coastal area, in which dissolved inorganic carbon (DIC) and dissolved organic carbon (DOC) account for more than 70% (Zhang et al., 2013). Many studies were conducted to investigate the carbon cycle in the Pearl River Estuary (He et al., 2010; Su et al., 2017; Liang et al., 2020). The Guangdong-HongKong-Macao GBA, one of the significant bay development areas alongside New York, San Francisco (United States), and Tokyo (Japan), is a highly developed and urbanized region in China. With the rapid economic development and urbanization in the GBA, the regional water environment has been affected seriously by human activities. For instance, Liu et al. (2020) showed that the organic C/N ratio in the Pearl River decreased from 11.8 to 5.0 after the river passed through several big cities. Such variations in nutrient/carbon flux and composition will change the carbon cycle (e.g., stimulating new primary production and enhancing biological pump efficiency) in coastal oceans, and have a significant implication for estimating coastal carbon budgets (Liu et al., 2020; Ye et al., 2021).

Submarine groundwater discharge, an important part of the hydrological cycle, is an invisible pathway of materials (i.e., nutrients, metals, and rare earth elements) into the ocean (Moore et al., 2008; Johannesson et al., 2011; Kim et al., 2011; Luo and Jiao, 2016; Rodellas et al., 2017; Wang et al., 2018; Zhang et al., 2020). The latest study including more than 200 coastal sites worldwide shows that SGD delivers more nutrients (nitrogen, phosphorus, and silicon) than rivers in most (~60%) of the coastal areas studied (Santos et al., 2021). The study finds that SGD-driven nutrients can enhance primary productivity, fish production, or coral calcification, but on the other hand, can lead to eutrophication of coastal waters, algal blooms or hypoxia events. Therefore, SGD can be regarded as an important indicator of the functioning and vulnerability of coastal ecosystems and is of great significance to the survival and maintenance of coastal societies at local and regional scales, even more at a global scale (Sawyer et al., 2016; Michael et al., 2017; Cho et al., 2018; Alorda-Kleinglass et al., 2021).

Similar to rivers, SGD also carries carbon into the oceans and plays an important role in the marine carbonate system (Cole et al., 2007; Liu et al., 2012; Stewart et al., 2015). A growing number of scientists have devoted more intensive attention to this aspect in recent years. Many studies investigated SGD-derived carbon flux [e.g., total alkalinity (TA), DIC] in different systems such as mangrove, estuary, salt marsh, and embayment (Liu et al., 2014, 2017; Sadat-Noori et al., 2016; Chen et al., 2018; Xiao et al., 2020; Dai et al., 2021; Wu et al., 2021). In the northern South China Sea, Liu et al. (2012) and Dai et al. (2021) estimated the SGD-derived DIC fluxes in different scales and they found that SGD is an important contributor to DIC. However, the effects of SGD on the marine carbon budgets are usually ignored in most studies (Liu et al., 2018; Ye et al., 2021; Yu et al., 2021) since it usually occurs below the seawater surface and is almost invisible and highly variable. In addition, the study

on the SGD-derived carbon in the GBA is very limited. Thus, understanding the contribution of both SGD and river to carbon cycle is of great significance to environmental assessment and management in the region.

The objectives of this study were to evaluate the carbon flux supplied by SGD and river, and reveal their potential impacts on the marine carbon cycles. Firstly, SGD-derived nitrate (NO_3^-) and carbon (DOC, DIC) fluxes were estimated using radium isotopes (^{224}Ra, ^{223}Ra, and ^{228}Ra) as tracers. Then the importance of SGD and river discharges on the carbon budget and their contributions to the new production and carbon cycling were discussed. Finally, two conceptual models were proposed illustrating the major potential processes of the carbon cycle induced by SGD and river discharges.

MATERIALS AND METHODS

Study Area

The GBA, with a total land area of ~56,000 km^2 (including nine cities in Guangdong province and two Special Administrative regions: HongKong and Macao) and a coastal length of ~1,480 km, is located in the northern South China Sea (**Figure 1**). There are one important estuary in southern China (Pearl River Estuary) and many important bays including Daya Bay, Dapeng Bay as well as Tolo Harbor in HongKong. The Pearl River, with an annual runoff of 3.26×10^{11} m^3/yr and suspended particles matter (SPM) load of 5.0×10^{10} g/d, is the largest river into the South China Sea through eight outlets (Wang et al., 2021). During the dry winter season, the coastal current flows from northeast to southwest, and the Pearl River flow turns to the west. Rainfall in this region is abundant and occurs mostly (80%) during the wet summer season (from April to September).

Sample Collection and Measurements

Fieldwork was carried out during the dry winter season (January 6–13, 2020, **Supplementary Table 1**). The sampling sites within 30 seawater from three transects (A1, A2, and A3), 24 coastal groundwater, and 7 rivers are shown in **Figure 1**. Water samples for radium extraction were collected in a large volume (60 L for seawater, 30 L for river water, ~5 L for coastal groundwater) and drained slowly (<1 L/min) through manganese-coated acrylic fiber (Mn-fiber) that absorb dissolved radium from water (Moore, 1976). Nitrate samples were filtered through 0.45 µm filters and collected with 45 ml Nalgene sampling bottles. DIC and DOC samples were filtered through 0.22 µm filter membranes, poisoned with HgCl and H$_3$PO$_4$ solution, respectively, and stored in 45 mL sampling vials. These samples were refrigerated at 4°C before analysis. The values of pH, oxidation-reduction potential (ORP), and salinity in water were immediately measured *in situ* using a multi-parameter water quality analyzer (HI9829T, HANA).

^{224}Ra, ^{223}Ra, and ^{228}Ra were detected by radium delayed coincidence counting system (RaDeCC; Moore, 2008). The uncertainties for radium measurements were 7% for ^{224}Ra and ^{228}Ra, and 12% for ^{223}Ra. Analyses for nitrate were carried out colorimetrically using a flow injection analyzer

FIGURE 1 | (A) The location of the Greater Bay Area in China, and **(B)** the sampling sites of groundwater, river water, and seawater.
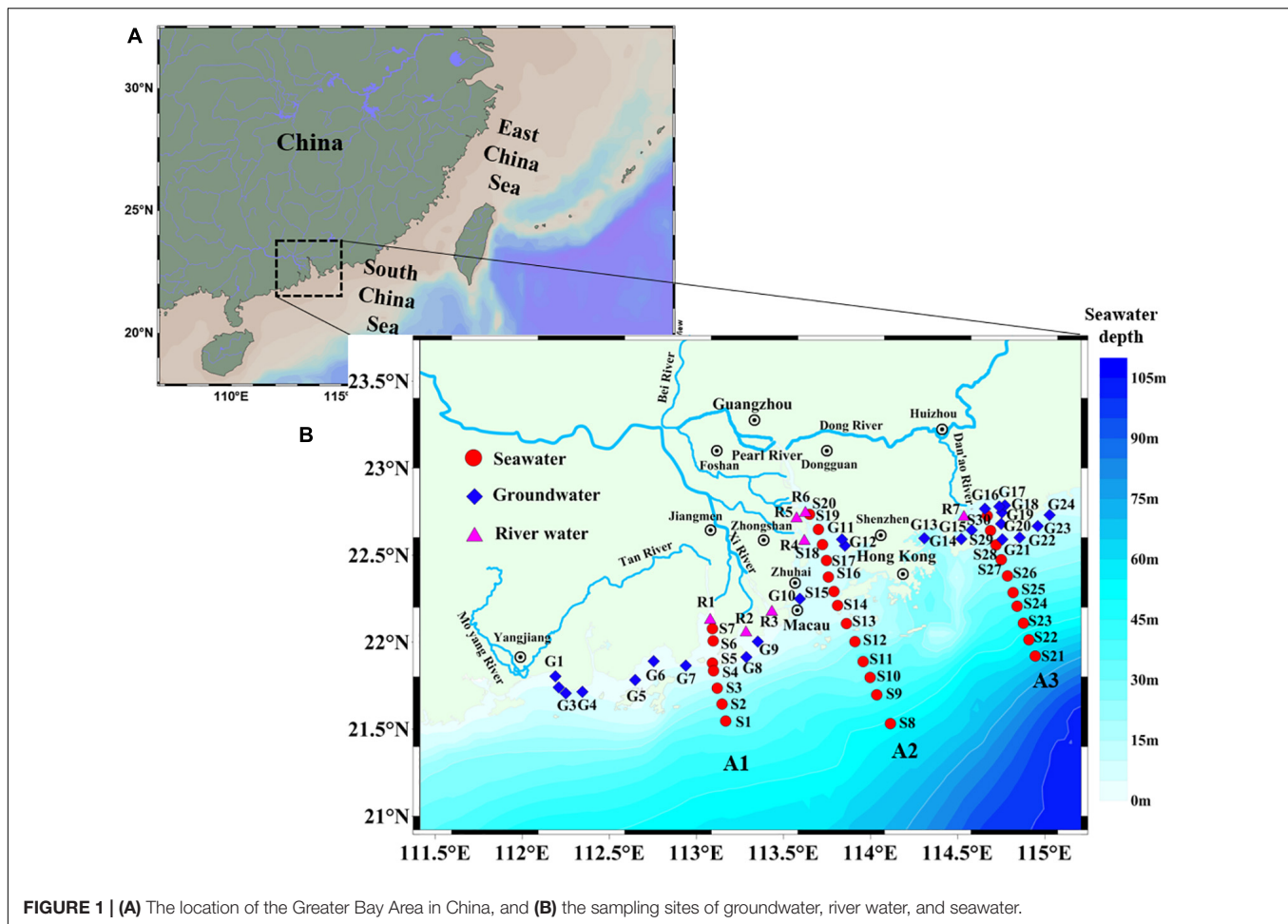
(FIA) with a detection limit of 5 µg/L (HACH QC8500, American). DOC and DIC were determined by a Total Organic Carbon/Nitrogen analyzer (Multi N/C 3100 Analyzer, Germany). The uncertainties of DOC and DIC concentration were better than 3%.

Submarine Groundwater Discharge-Derived Solute Fluxes Based on ²²⁸Ra Tracing Model

Radium isotopes (²²⁴Ra, ²²³Ra, ²²⁸Ra, and ²²⁶Ra), with the half-life from 3.6 days to 1,600 years, are widely used to trace SGD fluxes at different scales because of their enrichment in SGD (Rodellas et al., 2015; Wang et al., 2015; Zhang et al., 2016). Garcia-Orellana et al. (2021) summarized the application of radium isotopes tracing SGD and associated solute fluxes. Three models, radium mass balance model, radium endmember mixing model, and eddy diffusive mixing model, are usually applied to estimate SGD fluxes. The basic strategies of these models to estimate SGD is to determine first the radium flux supplied by SGD, and subsequently convert it into SGD flux by characterizing the groundwater radium endmember. Radium mass balance model which considers all the potential radium sources and sinks is the most widely used (Moore et al., 2008; Wang et al., 2018).

The eddy diffusive mixing model used in this study is suitable for open coastal systems.

The long-lived ²²⁸Ra was used to assess SGD flux into the GBA. The total input of ²²⁸Ra in the system is mainly controlled by SGD and river discharges; the input from sediments is negligible due to the long half-life of ²²⁸Ra. Thus SGD-derived ²²⁸Ra (F_{SGD}^{Ra-228}) can be calculated by subtracting riverine ²²⁸Ra (F_{R}^{Ra-228}) from the total input (F_{Total}^{Ra-228}) (Eq. 1a). The ²²⁸Ra flux attributed to river was calculated as the product of the activity of ²²⁸Ra (C_{R-i}^{Ra-228}) in the river and the corresponding river discharge (Q_{R-i}) (Eq. 1b). The total ²²⁸Ra input to the system was balanced by the offshore export of ²²⁸Ra, which was calculated as the product of the eddy diffusion coefficient (K_h), the offshore gradient of ²²⁸Ra (g_{Sea}^{Ra-228}), and the cross-sectional area (A) of the system (Eq. 1c).

$$F_{SGD}^{Ra-228} = F_{Total}^{Ra-228} - F_{R}^{Ra-228} \qquad (1a)$$

$$F_{R}^{Ra-228} = \sum_{i=1}^{n} Q_{R-i} C_{R-i}^{Ra-228} \qquad (1b)$$

$$F_{Total}^{Ra-228} = K_h g_{Sea}^{Ra-228} A \qquad (1c)$$

where K_h can be determined by an advection-diffusion model of short-lived ^{224}Ra and ^{223}Ra; n is the number of rivers in the region. The ^{224}Ra and ^{223}Ra distribution can be described as follows if ignoring the advection (Hancock et al., 2006; Wang et al., 2021):

$$-\frac{\partial}{\partial x}\left[K_h D\frac{\partial C_{Sea}^{Ra}}{\partial x}\right] + \lambda D C_{Sea}^{Ra} = B \tag{2a}$$

where C_{Sea}^{Ra} is ^{224}Ra or ^{223}Ra activity in seawater (dpm/100 L), x and D are offshore distance and seawater depth (m), respectively; l is the decay constant of ^{224}Ra or ^{223}Ra (d^{-1}), and B is the sedimentary radium flux [dpm/(m^{2}d)]. The boundary conditions, the radium fluxes across the coastline ($x = 0$) to be F_0 and at the shelf edge ($x = x_e$) to be $\lim_{x \to x_e} \frac{\partial C_{Sea}^{Ra}}{\partial x} = 0$, were given to solve this equation. Integration of Eq. 2a with respect to x yields:

$$-\left[K_h D\frac{\partial C_{Sea}^{Ra}}{\partial x}\right]_{x=0}^{x_e} = \int_{x=0}^{x_e}\left(B - \lambda D C_{Sea}^{Ra}\right)\,dx \tag{2b}$$

$$F_0 = \int_{x=0}^{x_e}\left(\lambda D C_{Sea}^{Ra} - B\right)\,dx \tag{2c}$$

The values of K_h can be determined when we obtained optimal agreement between measured and modeled radium activities (^{224}Ra and ^{223}Ra) for each transect. SGD-derived nitrate or carbon flux (F_N) is commonly calculated by multiplying the SGD flux (Q_{SGD}) by the concentration of nitrate or carbon in coastal groundwater (Wang et al., 2020). It can be represented by the following equation:

$$F_N = C_N Q_{SGD} = C_N \frac{F_{SGD}^{Ra-228}}{C_{GW}^{Ra-228}}$$
$$= \frac{C_N}{C_{GW}^{Ra-228}}\left(K_h g_{Sea}^{Ra-228} A - \sum_{i=1}^{n} Q_{R-i} C_{R-i}^{Ra-228}\right) \tag{3}$$

where C_N and C_{GW}^{Ra-228} are solute (nitrate, DOC, and DIC) concentration and ^{228}Ra activity in coastal groundwater, respectively.

The common method to estimate SGD-derived solute (nitrate and carbon) fluxes is to calculate first the SGD flux by dividing SGD-associated radium flux by radium activity in groundwater (i.e., radium endmember), and then multiply the SGD flux by solute concentration in groundwater (i.e., solute endmember). During this process, the determination of the two endmembers is usually major source of uncertainty for the final SGD-derived solute fluxes because of the spatial and temporal variability of radium and solutes in groundwater (Michael et al., 2011; Waska et al., 2019; Wang et al., 2020). To reduce the uncertainty of SGD-derived nitrate/carbon flux estimations, in this study, the term C_N/C_{GW}^{Ra-228} in Eq. 3 was regarded as a unified parameter to discuss later.

RESULTS

Radium Isotopes

The spatial distributions of radium (^{224}Ra, ^{223}Ra, and ^{228}Ra) and salinity in seawater and coastal groundwater are shown in **Figure 2**. In general, the high radium activity and low salinity occurred in the nearshore area, whereas the low radium activity and high salinity occurred in the offshore area. Seawater salinity ranged from 14.49 to 34.99 PSU (Practical Salinity Unit) and it was very low in the western nearshore area resulting from the Pearl River freshwater dilution (**Figure 2D**). The radium activity of seawater ranged from 11.72 to 113.72 dpm/100 L for ^{224}Ra, from 0.15 to 4.76 dpm/100 L for ^{223}Ra, and from 8.04 to 80.41 dpm/100 L for ^{228}Ra (**Supplementary Table 1**). Coastal groundwater, however, had very high radium activity within ^{224}Ra: 0.81–119.2 dpm/100 L, ^{223}Ra: 0.05–4.10 dpm/100 L, and ^{228}Ra: 0.17–34.46 dpm/100 L (**Supplementary Table 2**). As shown in **Figure 3**, ^{224}Ra had a strong linear relationship with ^{223}Ra and ^{228}Ra in both coastal groundwater and seawater. The coastal groundwater with high Ra activities and ratios (^{224}Ra/^{223}Ra and ^{224}Ra/^{228}Ra) was the main source of radium in the ocean.

Nitrate and Carbon

Solute concentrations of coastal groundwater ranged from 0.005 to 3.17 mg/L with a median of 0.19 mg/L for NO_3^-, from 1.00 to 7.83 mg/L with a median of 1.34 mg/L for DOC, and from 4.58 to 31.49 mg/L with a median of 13.56 mg/L for DIC. For the river water samples, solute concentrations ranged from 0.69 to 4.36 mg/L with a median of 1.22 mg/L for NO_3^-, from 1.08 to 1.82 mg/L with a median of 1.23 mg/L for DOC, and 9.50 mg/L for DIC (**Figure 4** and **Supplementary Table 3**). The highest concentration of NO_3^- (4.36 mg/L) and DOC (1.82 mg/L) occurred in the Dan'ao River (R7) which suffered serious environmental pollution from high-intensity human activities (Wang et al., 2021). Solute concentrations in both coastal groundwater and river water are ranked as DIC>DOC>NO_3^-. Nitrate concentrations in coastal groundwater are less than that in river water, while carbon contents in coastal groundwater are slightly greater than that in river water (**Figure 4**).

Submarine Groundwater Discharge-Derived Solute Fluxes

Eddy Diffusion Coefficient

In this study, the eddy diffusion coefficient was estimated by using Eq. 2. All the values used in the Eq. 2 are shown in **Table 1**. Based on the observed data, seawater depth (D) can be described by a linear relationship with offshore distance (x): $D = 5.84 \times 10^{-4} x$ for A1, $D = 3.58 \times 10^{-4} x$ for A2, and $D = 5.43 \times 10^{-4} x$ for A3 (**Table 1**). The optimal agreement between measured and modeled radium activities, as illustrated in **Figure 5**, was obtained within the application of the short-lived ^{224}Ra and ^{223}Ra diffusive model (Eq. 2). The eddy diffusion coefficients K_h derived from ^{224}Ra are 114.8 km^2/d for A1, 365.4 km^2/d for A2, and 110.2 km^2/d for A3, and derived from ^{223}Ra are 30.4 km^2/d for A1, 139.3 km^2/d for A2, and 36.7 km^2/d for A3 (**Table 1**). The
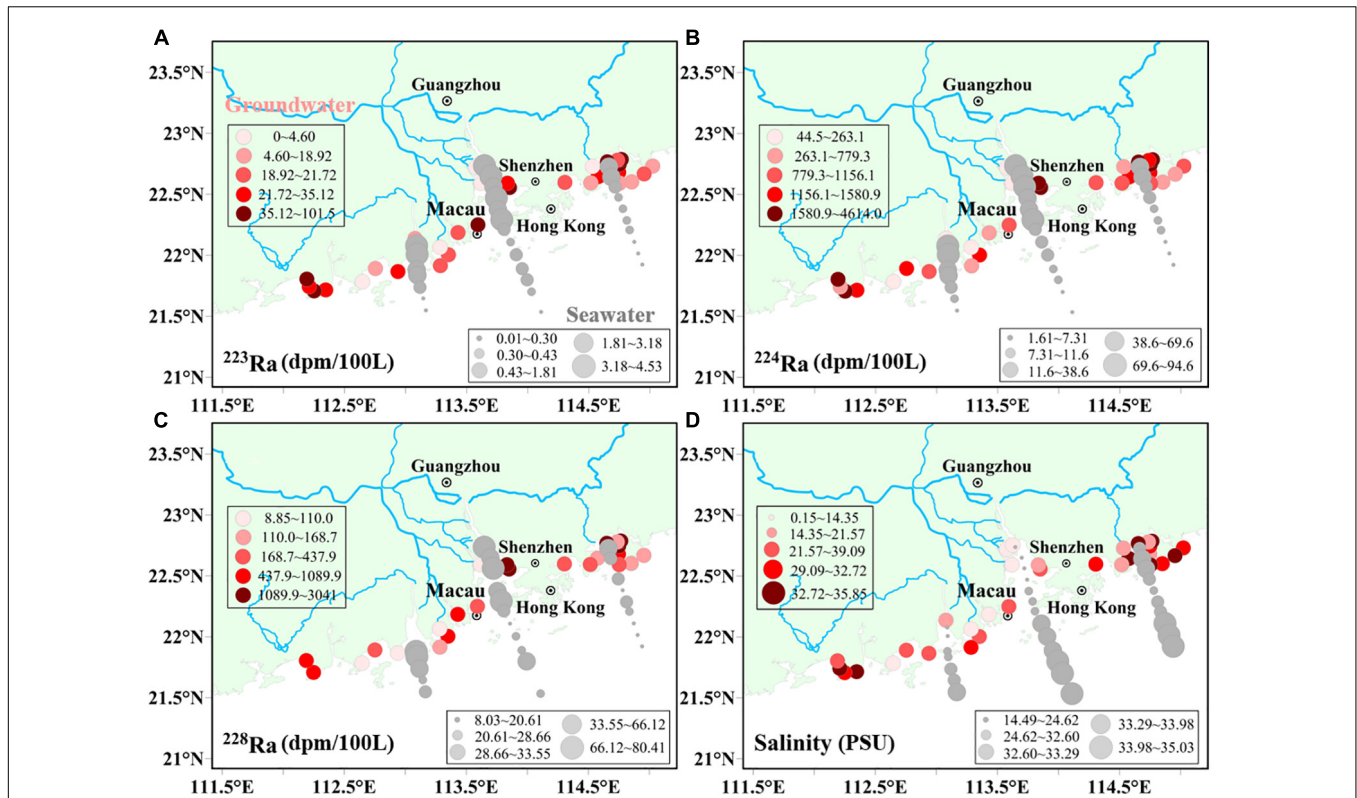
FIGURE 2 | Distributions of panel **(A)** ^{223}Ra, **(B)** ^{224}Ra, **(C)** ^{228}Ra, and **(D)** salinity in seawater (gray dots) and coastal groundwater (red dots) of the Greater Bay Area (GBA).
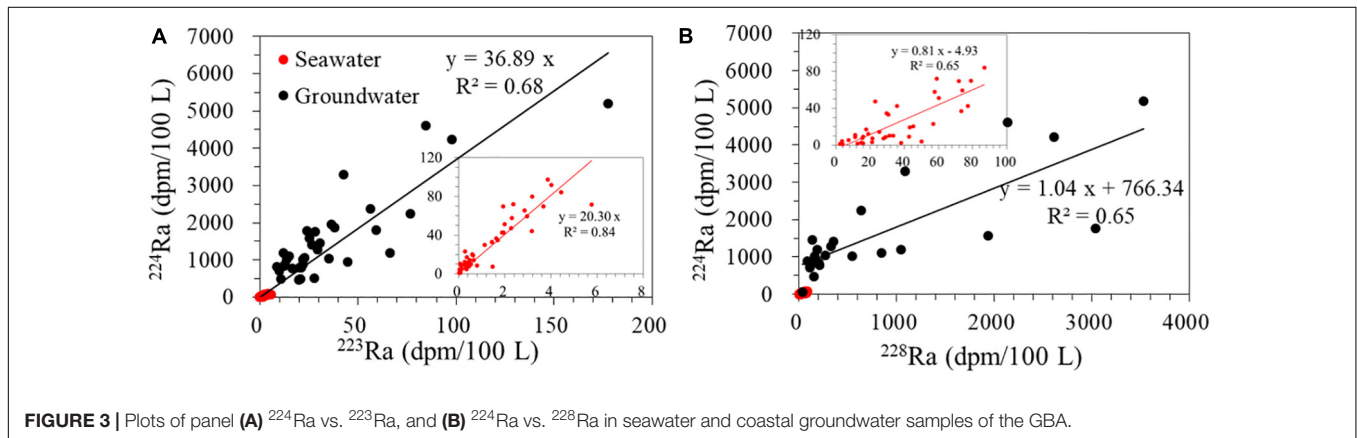
FIGURE 3 | Plots of panel **(A)** ^{224}Ra vs. ^{223}Ra, and **(B)** ^{224}Ra vs. ^{228}Ra in seawater and coastal groundwater samples of the GBA.

values of K_h derived from ^{223}Ra are less than that from ^{224}Ra which usually presents an accurate estimation for K_h (Li and Cai, 2011; Wang et al., 2021).

Submarine Groundwater Discharge-Derived Nitrate and Carbon Fluxes Based on Radium Model

The total ^{228}Ra flux to the system (Eq. 1c) was calculated to be 6.13×10^{12} dpm/d based on the derived K_h (**Table 1**) and the linear gradient of ^{228}Ra (**Figure 6A**) at three transects. The riverine ^{228}Ra flux (Eq. 1b) was estimated to be 1.68×10^{12} dpm/d, which includes dissolved in the water

and desorbed from SPM (**Supplementary Table 4**). Thus SGD-derived solute fluxes (Eq. 3) were calculated to be $(0.73–16.4) \times 10^8$ g/d with a median of 2.06×10^8 g/d for NO_3^-, $(0.60–9.94) \times 10^9$ g/d with a median of 2.25×10^9 g/d for DOC, and $(0.77–3.29) \times 10^{10}$ g/d with a median of 1.66×10^{10} g/d for DIC. Here the ranges of $NO_3^-/^{228}$Ra, DOC/^{228}Ra, and DIC/^{228}Ra ratios between the first and third quartiles of the coastal groundwater dataset (**Figure 6B**) were used in Eq. 3. A previous study suggested that the sources of SGD-derived nitrate in the GBA were natural soil and anthropogenic discharge (Wang et al., 2021). SGD is a mixture of terrestrial freshwater

FIGURE 4 | Concentrations of nitrate (NO_3^-), dissolved organic carbon (DOC), and dissolved inorganic carbon (DIC) in coastal groundwater and river water samples.
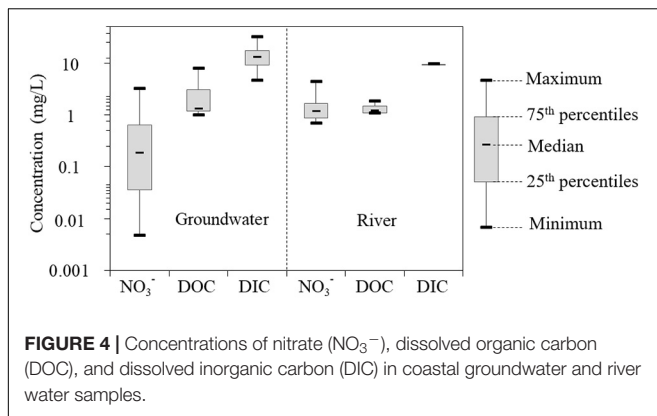
and circulated seawater. The circulated seawater, accounting for a large part of SGD, is important for the delivery of solutes from land to the ocean.

Riverine Nitrate and Carbon Fluxes

The nitrate and carbon fluxes *via* rivers into the GBA were calculated as the product of the concentrations of nitrate and carbon in the river and the corresponding river discharge. In the GBA, the Pearl River is the dominant river with a flux of 8.92×10^8 m^3/d and a mean concentration of 1.01 mg/L for NO_3^-, 1.18 mg/L for DOC, and 9.50 mg/L for DIC. Thus, the riverine NO_3^-, DOC, and DIC inputs were estimated to be 8.82×10^8 g/d, 1.05×10^9 g/d, and 8.48×10^9 g/d, respectively. Numerous studies have well-investigated cycles of nitrogen and carbon and their seasonality within the Pearl River and adjacent waters (Lu et al., 2009; He et al., 2010; Liu et al., 2020; Xuan et al., 2020; Ye et al., 2021). Liu et al. (2020) investigated the spatial distribution of organic carbon and nitrogen in the Pearl River. They found that both DOC and total organic nitrogen (TON) were increased from upstream to downstream, with an increase of five times for TON and two times for DOC in the dry season. The nitrogen and carbon fluxes from the current study are consistent with previous findings.

DISCUSSION

Variability of Nitrate Fluxes and K_h

Wang et al. (2021) quantified nitrate fluxes from SGD and rivers into the GBA in the wet summer season with values of $(5.28 \pm 0.73) \times 10^8$ g/d and 1.32×10^9 g/d, respectively. It can

be found that nitrate fluxes from SGD and river to the GBA were greater in the wet summer season than in the dry winter season. This is the less discharge of river and groundwater during the dry season, which can be supported by the seawater salinity and pH distributions in the seawater. **Figure 7** shows seawater salinity and pH in the dry and wet seasons. Both salinity and pH were less in the wet summer season than in the dry winter season, which indicated directly the decrease of terrestrial freshwater including river water and fresh groundwater.

The eddy diffusion coefficients for the GBA in the summer season were estimated by Wang et al. (2021) using the same method. The summer eddy coefficient was 21.04 km^2/d for A1 transect, 88.4 km^2/d for A2 transect, and 11.76 km^2/d for A3 transect (Wang et al., 2021). The winter eddy coefficient determined in this study is about 4–10 times greater than the summer eddy coefficient. During the winter, the strong current will enhance horizontal mixing and result in relatively higher values for eddy mixing. Among three transects (A1–A3), A2 has the highest values of eddy diffusion coefficient during both summer and winter seasons. Transect A2 is the longest one and is more influenced by terrestrial freshwater (Pearl River). The force of Pearl River discharge could enhance horizontal mixing and thus create a relatively higher value of eddy diffusion coefficient. In addition, differences in scale can produce some of the variances in the eddy diffusion coefficient. The eddy diffusion term usually becomes larger at greater length scales (Moore, 2000).

Effects of Submarine Groundwater Discharge and River on Coastal Carbon System

Regarding carbon flux, it can be found that SGD-derived DOC and DIC fluxes are ~2 times as great as riverine input, but SGD-derived NO_3^- flux is one-fourth of the riverine input. Anthropogenic input of nitrogen is the primary determinant of NO_3^- accumulation in the Pearl River (Xuan et al., 2020). DIC is the dominant form of carbon in SGD, and DOC concentration is below one-tenth of DIC in most groundwater samples (except for two sites, **Figure 8A**). The relationship between DOC and the residual NO_3^- is shown that DOC concentrations decreased while dissolved NO_3^- concentrations increased (**Figure 8B**). This observation revealed that DOC could be consumed by biological production when they transport from land to sea. Waska et al. (2021) also found that the subterranean estuary is a net sink of terrestrial organic carbon. SGD-derived DIC and DOC have been reported in some coastal systems worldwide

TABLE 1 | Values used in ^{224}Ra and ^{223}Ra advection-diffusion equation.

Parameters	^{224}Ra diffusive model			^{223}Ra diffusive model		
	A1	A2	A3	A1	A2	A3
λ (d^{-1})		0.189			0.0606	
B[dpm/(m^{2}d)]		156.5			2.12	
D (m)	5.84×10^{-4}	3.58×10^{-4}	5.43×10^{-4}	5.84×10^{-4}	3.58×10^{-4}	5.43×10^{-4}
K_h (km^2/d)	114.8	365.4	110.2	30.4	139.3	36.7
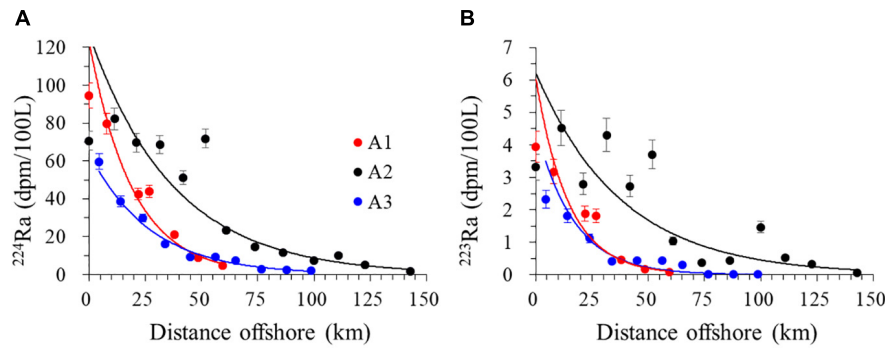
FIGURE 5 | Plots of panel **(A)** ^{224}Ra and **(B)** ^{223}Ra activity vs. distance offshore at three transects A1–A3; the dots and lines are the measured and modeled radium activities, respectively.
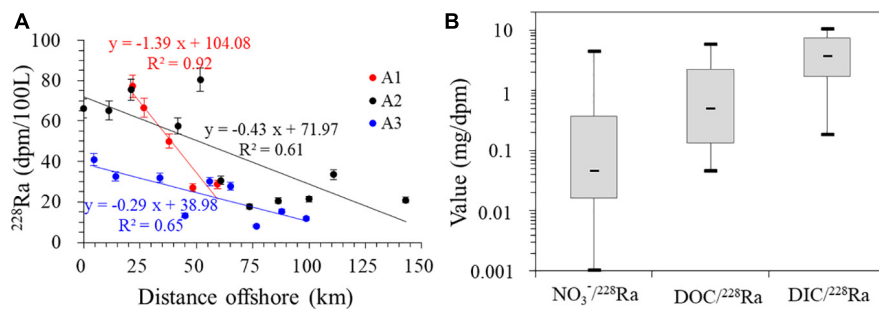
FIGURE 6 | Plots of panel **(A)** seawater ^{228}Ra activity vs. distance offshore at three transect A1–A3, and **(B)** the ratio of $NO_3^-/^{228}$Ra, $DOC/^{228}$Ra, and $DIC/^{228}$Ra in coastal groundwater.
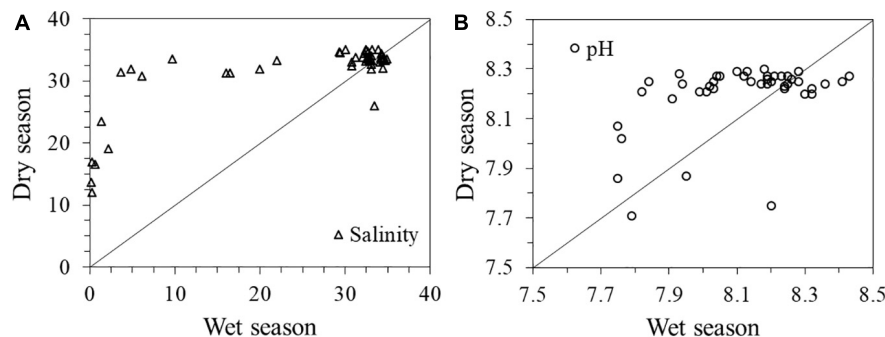
FIGURE 7 | Plots of seawater **(A)** salinity, and **(B)** pH in the wet season vs. in the dry season.

such as Okatee Estuary, South Carolina, United States (Moore et al., 2006), Southwest Florida Shelf, United States (Liu et al., 2014), and Northern South China Sea (Tan et al., 2018). These findings suggested that SGD is a dominant source of DIC and DOC to coastal waters and may contribute significantly to coastal carbon budgets.

Submarine groundwater discharge-derived and riverine NO_3^- into the GBA can stimulate new primary production and enhance biological pump efficiency. Using the Redfield ratio of C/N = 106:16 to derive primary production in terms of carbon uptake, estimated potential primary production

by SGD and river were 1.17×10^9 g C/d and 5.01×10^9 g C/d, which were 7.1 and 59.1% of SGD-derived and riverine DIC, respectively. The new primary production rates supplied by SGD showed a similar range to the study in the Daya Bay [i.e., 54–73 mg C/(m^{2}d)], an important bay in the GBA (Wang et al., 2018).

Submarine groundwater discharge-derived and riverine DOC, once entering the coastal sea within the environment of sufficient inorganic nitrogen, could be easily consumed by biological production and thus cannot be stored as inert organic carbon. If assuming that 80% of the flux of SGD-derived and riverine DOC
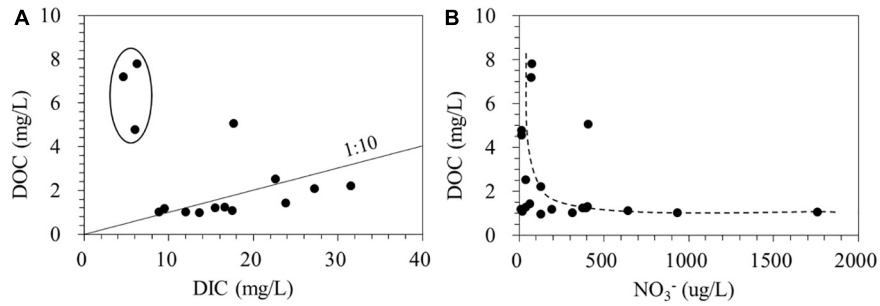
FIGURE 8 | Plots of concentrations **(A)** DOC vs. DIC, and **(B)** DOC vs. NO_3^- in coastal groundwater samples.
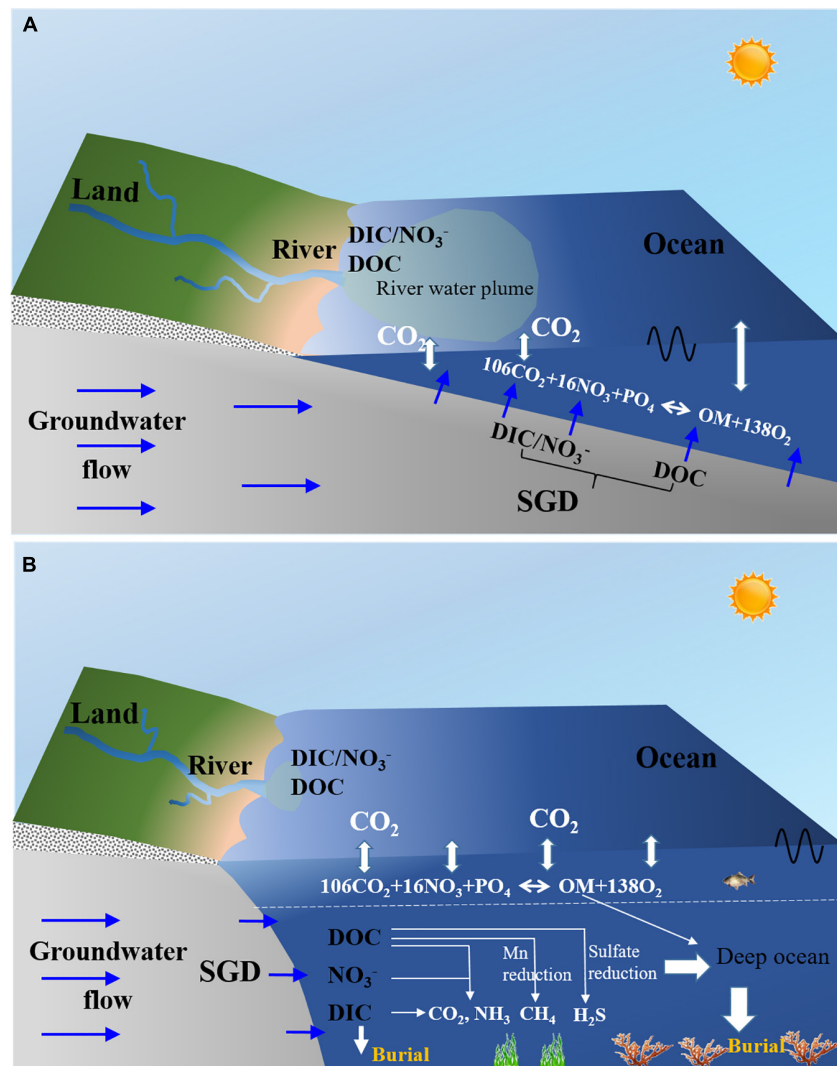
FIGURE 9 | Schematic of the processes of submarine groundwater discharge (SGD) and riverine nitrate and carbon to the ocean on **(A)** near shore scale with shallow water, and **(B)** shelf scale with deep water.

will be remineralized, the remineralization process can produce CO_2 of 1.80×10^9 g C/d and 0.84×10^9 g C/d, respectively. The remineralization of SGD-derived DOC usually occurs at the

bottom of the ocean which will potentially result in hypoxia and acidification at the bottom water body. Combined with the processes of nitrate and DOC, SGD is a potential net source

of atmospheric CO_2 with a flux of 0.63×10^9 g C/d, while river is a potential net sink of atmospheric CO_2 with a flux of 4.17×10^9 g C/d. Previous studies in the Pearl River Estuary (Wu et al., 2017) and other river-dominated systems (Bauer et al., 2013; Guo et al., 2015) have often observed the net production of DOC in the river plume.

The input of land DIC mainly affects the balance of the carbonate system in marine water. Compared with seawater, SGD and river water have lower pH values, which suggests that much more CO_2 could be dissolved in SGD and river water. Charbonnier et al. (2022) also found that terrestrial groundwater contains a lot of CO_2 and is an important contributor to the DIC flux to the coastal ocean. When SGD and river discharge to the ocean, the balance of the carbonate system may be changed resulting in enhancement of calcium carbonate or CO_2 exchange with the atmosphere. If assuming that the free CO_2 in SGD-derived and riverine DIC can escape to the atmosphere from water body. Based on pH values (**Supplementary Table 2**), the free CO_2 was estimated to be 5% of DIC. Thus, SGD-derived and riverine DIC would potentially supply atmospheric CO_2 of 0.83×10^9 g C/d and 0.42×10^9 g C/d, respectively.

Indeed, marine carbon cycles are influenced by the combination of terrigenous NO_3^-, DOC, and DIC. Based on the above discussion, we conclude that SGD in the studied system is a potential net source of atmospheric CO_2 with a flux of 1.46×10^9 g C/d and river is a potential net sink of atmospheric CO_2 with a flux of 3.75×10^9 g C/d. Their coupled effect on ocean suggests that SGD and river would potentially enhance CO_2 exchange flux from atmospheric to ocean in the dry winter season and they play a significant role in the carbon cycles of GBA.

Conceptual Model for Carbon Process

Submarine groundwater discharge and river water usually have different physical and chemical characteristics, such as the long water residence times, strong water-rock interaction, and complex biogeochemical processes in groundwater flow. Therefore, the composition and structure of chemical materials in river water and groundwater discharged into the ocean are quite different. Generally, the discharged river water has high oxygen and nutrient concentrations and forms freshwater plumes on the ocean surface. Groundwater discharged into the sea from the seabed with a low flow rate, on the other hand, has a low oxygen content and high nutrient concentrations (Slomp and Van Cappellen, 2004; Kim et al., 2017; Waska et al., 2021). Thus they present different processes in marine carbon cycles. Here two conceptual models, as shown in **Figure 9**, were proposed to illustrate the major potential processes of the carbon cycle induced by SGD and river discharges.

Figure 9A shows the contributions of SGD and river discharges to the carbon system on the nearshore scale with shallow oceans. In this case, the bottom water can easily exchange with upper water and air. Thus CO_2 produced from SGD processes (e.g., remineralization of SGD-derived DOC) can escape to the atmosphere. On the other hand, the consumption of CO_2 in SGD processes (e.g., new primary production by

SGD-derived nitrate) can achieve from the atmosphere. Other products from SGD can participate in other processes of the carbon cycle in shallow seawater. Overall, a significant amount of nitrate, DOC, and DIC stimulate phytoplankton blooms in the upper water and consume oxygen in the bottom water, resulting in coastal hypoxia (Su et al., 2017).

Figure 9B shows the contributions of SGD and river discharges to the carbon system on the shelf scale with deep oceans. In this case, the bottom water is in a reducing environment and hardly exchange with upper water and air. Thus the high-carbon water masses usually occur in the bottom resulting from the input of SGD-derived nitrate and carbon. The carbon in these high-carbon water masses deposited or moved into deeper waters and finally deposited and sealed. This demonstrated that SGD can be regarded as a sink of carbon in a sense. In the upper water, only a fraction of the organic carbon produced by the river was transported to the deep ocean and stored there.

CONCLUSION

In this study, both SGD and river-derived nitrate and carbon fluxes and their impacts on the carbon cycle were investigated in the GBA, China. SGD-derived NO_3^-, DOC, and DIC fluxes were estimated to be $(0.73–16.4) \times 10^8$ g/d, $(0.60–9.94) \times 10^9$ g/d, and $(0.77–3.29) \times 10^{10}$ g/d, respectively. The riverine NO_3^-, DOC, and DIC inputs were estimated to be 8.82×10^8 g/d, 1.05×10^9 g/d, and 8.48×10^9 g/d, respectively. These additional fluxes are of significance to stimulate new primary production and affect the balance of the carbonate system in marine water. We found that SGD is a potential net source of atmospheric CO_2 with a flux of 1.46×10^9 g C/d in the dry winter season of the study area. However, river is a potential net sink of atmospheric CO_2 with a flux of 3.75×10^9 g C/d. The findings of this study suggest that SGD, as important as rivers, plays a significant role in the carbon cycles but has long been ignored in the coastal carbon budgets because of its invisible and highly variable. In this study, we just considered the dissolved form of nitrogen and carbon and ignored the particulate form. A few studies have shown that particulate form is an important portion of total carbon flux (Huang et al., 2017). Overall, both SGD and river should be considered in assessing carbon budgets at regional and global scales future.

DATA AVAILABILITY STATEMENT

The original contributions presented in the study are included in the article/**Supplementary Material**, further inquiries can be directed to the corresponding authors.

AUTHOR CONTRIBUTIONS

XW designed the study and wrote the original draft preparation. YZ contributed to the manuscript writing, sample measurements,

and data analysis. CZ reviewed and edited the manuscript and acquired funding. MHL, SY, and MQL conducted the fieldwork and sample measurements. HL contributed to the study design and data analysis. All authors approved the submitted version.

SUPPLEMENTARY MATERIAL

The Supplementary Material for this article can be found online at: https://www.frontiersin.org/articles/10.3389/fmars.2021.817001/full#supplementary-material

REFERENCES

Alorda-Kleinglass, A., Ruiz-Mallén, I., Diego-Feliu, M., Rodellas, V., Bruach-Menchén, J. M., and Garcia-Orellana, J. (2021). The social implications of submarine groundwater discharge from an ecosystem services perspective: a systematic review. *Earth-Sci. Rev.* 221:103742. doi: 10.1016/j.earscirev.2021.103742

Bauer, J. E., Cai, W. J., Raymond, P. A., Bianchi, T. S., Hopkinson, C. S., and Regnier, P. A. (2013). The changing carbon cycle of the coastal ocean. *Nature* 504, 61–70. doi: 10.1038/nature12857

Cai, W. J. (2011). Estuarine and coastal ocean carbon paradox: CO_2 sinks or sites of terrestrial carbon incineration? *Annu. Rev. Mar. Sci.* 3, 123–145. doi: 10.1146/annurev-marine-120709-142723

Charbonnier, C., Anschutz, P., Abril, G., Mucci, A., Deirmendjian, L., Poirier, D., et al. (2022). Carbon dynamics driven by seawater recirculation and groundwater discharge along a forest-dune-beach continuum of a high-energy meso-macro-tidal sandy coast. *Geochim. Cosmochim. Acta* 317, 18–38. doi: 10.1016/j.gca.2021.10.021

Chen, X. G., Zhang, F. F., Lao, Y. L., Wang, X. L., Du, J. Z., and Santos, I. R. (2018). Submarine groundwater discharge-derived carbon fluxes in mangroves: an important component of blue carbon budgets? *J. Geophys. Res. Oceans* 123, 6962–6979. doi: 10.1029/2018jc014448

Cho, H. M., Kim, G., Kwon, E. Y., Moosdorf, N., Garcia-Orellana, J., and Santos, I. R. (2018). Radium tracing nutrient inputs through submarine groundwater discharge in the global ocean. *Sci. Rep.* 8:2439. doi: 10.1038/s41598-018-20806-2

Cole, J. J., Prairie, Y. T., Caraco, N. F., McDowell, W. H., Tranvik, L. J., Striegl, R. G., et al. (2007). Plumbing the global carbon cycle: integrating inland waters into the terrestrial carbon budget. *Ecosystems* 10, 172–185. doi: 10.1007/s10021-006-9013-8

Dai, G., Wang, G., Li, Q., Tan, E., and Dai, M. (2021). Submarine groundwater discharge on the western shelf of the northern south china sea influenced by the pearl river plume and upwelling. *J. Geophys. Res. Oceans* 126:e2020JC016859. doi: 10.1029/2020JC016859

Dai, M., Yin, Z., Meng, F., Liu, Q., and Cai, W. J. (2012). Spatial distribution of riverine DOC inputs to the ocean: an updated global synthesis. *Curr. Opin. Environ. Sustain.* 4, 170–178. doi: 10.1016/j.cosust.2012.03.003

Garcia-Orellana, J., Rodellas, V., Tamborski, J., Diego-Feliu, M., van Beek, P., Weinstein, Y., et al. (2021). Radium isotopes as submarine groundwater discharge (SGD) tracers: Review and recommendations. *Earth-Sci. Rev.* 220:103681.

Guo, X. H., Zhai, W. D., Dai, M. H., Zhang, C., Bai, Y., Xu, Y., et al. (2015). Air-sea CO_2 fluxes in the East China Sea based on multiple-year underway observations. *Biogeosciences* 12, 5495–5514. doi: 10.5194/bg-12-5495-2015

Hancock, G. J., Webster, I. T., and Stieglitz, T. C. (2006). Horizontal mixing of great barrier reef waters: offshore diffusivity determined from radium isotope distribution. *J. Geophys. Res.* 111:C12019. doi: 10.1029/2006JC003608

He, B., Dai, M., Zhai, W., Wang, L., Wang, K., Chen, J., et al. (2010). Distribution, degradation and dynamics of dissolved organic carbon and its major compound classes in the Pearl River estuary, China. *Mar. Chem.* 119, 52–64. doi: 10.1016/j.marchem.2009.12.006

Huang, T. H., Chen, C. T. A., Tseng, H. C., Lou, J. Y., Wang, S. L., Yang, L., et al. (2017). Riverine carbon fluxes to the South China Sea. *J. Geophys. Res. Biogeosci.* 122, 1239–1259. doi: 10.1002/2016jg003701

Johannesson, K. H., Chevis, D. A., Burdige, D. J., Cable, J. E., Martin, J. B., and Roy, M. (2011). Submarine groundwater discharge is an important net source of light and middle REEs to coastal waters of the Indian River Lagoon, Florida, USA. *Geochim. Cosmochim. Acta* 75, 825–843. doi: 10.1016/j.gca.2010.11.005

Kim, G., Kim, J. S., and Hwang, D. W. (2011). Submarine groundwater discharge from oceanic islands standing in oligotrophic oceans: Implications for global biological production and organic carbon fluxes. *Limnol. Oceanogr.* 56, 673–682.

Kim, K. H., Heiss, J. W., Michael, H. A., Cai, W. J., Laattoe, T., Post, V. E. A., et al. (2017). Spatial Patterns of Groundwater Biogeochemical Reactivity in an Intertidal Beach Aquifer. *J. Geophys. Res. Biogeosci.* 122, 2548–2562. doi: 10.1002/2017jg003943

Li, C., and Cai, W. (2011). On the calculation of eddy diffusivity in the shelf water from radium isotopes: high sensitivity to advection. *J. Mar. Syst.* 86, 28–33. doi: 10.1016/j.jmarsys.2011.01.003

Liang, B., Hu, J. T., Li, S. Y., Ye, Y. X., Liu, D. H., and Huang, J. (2020). Carbon system simulation in the pearl River Estuary, China: mass fluxes and transformations. *J. Geophys. Res. Biogeosci.* 125:20.

Liu, Q., Charette, M. A., Breier, C. F., Henderson, P. B., McCorkle, D. C., Martin, W., et al. (2017). Carbonate system biogeochemistry in a subterranean estuary – Waquoit Bay, USA. *Geochim. Cosmochim. Acta* 203, 422–439. doi: 10.1016/j.gca.2017.01.041

Liu, Q., Charette, M. A., Henderson, P. B., McCorkle, D. C., Martin, W., and Dai, M. (2014). Effect of submarine groundwater discharge on the coastal ocean inorganic carbon cycle. *Limnol. Oceanogr.* 59, 1529–1554. doi: 10.4319/lo.2014.59.5.1529

Liu, Q., Dai, M., Chen, W., Huh, C. A., Wang, G., Li, Q., et al. (2012). How significant is submarine groundwater discharge and its associated dissolved inorganic carbon in a river-dominated shelf system? *Biogeosciences* 9, 1777–1795. doi: 10.5194/bg-9-1777-2012

Liu, Q., Guo, X. H., Yin, Z. Q., Zhou, K. B., Roberts, E. G., and Dai, M. H. (2018). Carbon fluxes in the China Seas: An overview and perspective. *Sci. China Earth Sci.* 61, 1564–1582. doi: 10.1007/s11430-017-9267-4

Liu, Q., Liang, Y., Cai, W.-J., Wang, K., Wang, J., and Yin, K. (2020). Changing riverine organic C:N ratios along the Pearl River: implications for estuarine and coastal carbon cycles. *Sci. Total Environ.* 709:136052. doi: 10.1016/j.scitotenv.2019.136052

Lu, F. H., Ni, H. G., Liu, F., and Zeng, E. Y. (2009). Occurrence of nutrients in riverine runoff of the Pearl River Delta, South China. *J. Hydrol.* 376, 107–115. doi: 10.1016/j.jhydrol.2009.07.018

Luo, X., and Jiao, J. J. (2016). Submarine groundwater discharge and nutrient loadings in Tolo Harbor, Hong Kong using multiple geotracer-based models, and their implications of red tide outbreaks. *Water Res.* 102, 11–31. doi: 10.1016/j.watres.2016.06.017

Michael, H. A., Charette, M. A., and Harvey, C. F. (2011). Patterns and variability of groundwater flow and radium activity at the coast: a case study from Waquoit Bay, Massachusetts. *Mar. Chem.* 127, 100–114. doi: 10.1016/j.marchem.2011.08.001

Michael, H. A., Post, V. E. A., Wilson, A. M., and Werner, A. D. (2017). Science, society, and the coastal groundwater squeeze. *Water Resour. Res.* 53, 2610–2617. doi: 10.1002/2017wr020851

Moore, W. S. (1976). Sampling ^{228}Ra in the deep ocean. *Deep Sea Res. Oceanogr. Abs.* 23, 647–651. doi: 10.1016/0011-7471(76)90007-3

Moore, W. S. (2000). Determining coastal mixing rates using radium isotopes. *Continent. Shelf Res.* 20, 1993–2007. doi: 10.1016/j.jenvrad.2008.06.010

Moore, W. S. (2008). Fifteen years experience in measuring ^{224}Ra and ^{223}Ra by delayed-coincidence counting. *Mar. Chem.* 109, 188–197. doi: 10.1016/j.marchem.2007.06.015

Moore, W. S., Blanton, J. O., and Joye, S. B. (2006). Estimates of flushing times, submarine groundwater discharge, and nutrient fluxes to Okatee Estuary, South Carolina. *J. Geophys. Res.* 111:C09006. doi: 10.1029/2005JC003041

Moore, W. S., Sarmiento, J. L., and Key, R. M. (2008). Submarine groundwater discharge revealed by ^{228}Ra distribution in the upper Atlantic Ocean. *Nat. Geosci.* 1, 309–311. doi: 10.1038/ngeo183

Rodellas, V., Garcia-Orellana, J., Masque, P., Feldman, M., and Weinstein, Y. (2015). Submarine groundwater discharge as a major source of nutrients to the Mediterranean Sea. *Proc. Natl. Acad. Sci. U.S.A.* 112, 3926–3930. doi: 10.1073/pnas.1419049112

Rodellas, V., Garcia-Orellana, J., Trezzi, G., Masqué, P., Stieglitz, T. C., Bokuniewicz, H., et al. (2017). Using the radium quartet to quantify submarine groundwater discharge and porewater exchange. *Geochim. Cosmochim. Acta* 196, 58–73. doi: 10.1016/j.gca.2016.09.016

Sadat-Noori, M., Maher, D. T., and Santos, I. R. (2016). Groundwater discharge as a source of dissolved carbon and greenhouse gases in a subtropical estuary. *Estuaries Coasts* 39, 639–656. doi: 10.1007/s12237-015-0042-4

Santos, I. R., Chen, X., Lecher, A. L., Sawyer, A. H., Moosdorf, N., Rodellas, V., et al. (2021). Submarine groundwater discharge impacts on coastal nutrient biogeochemistry. *Nat. Rev. Earth Environ.* 2, 307–323. doi: 10.1016/j.marpolbul.2013.07.045

Sawyer, A. H., David, C. H., and Famiglietti, J. S. (2016). Continental patterns of submarine groundwater discharge reveal coastal vulnerabilities. *Science* 353, 705–707. doi: 10.1126/science.aag1058

Slomp, C. P., and Van Cappellen, P. (2004). Nutrient inputs to the coastal ocean through submarine groundwater discharge: controls and potential impact. *J. Hydrol.* 295, 64–86. doi: 10.1016/j.scitotenv.2011.09.088

Stewart, B. T., Santos, I. R., Tait, D. R., Macklin, P. A., and Maher, D. T. (2015). Submarine groundwater discharge and associated fluxes of alkalinity and dissolved carbon into Moreton Bay (Australia) estimated via radium isotopes. *Mar. Chem.* 174, 1–12. doi: 10.1016/j.marchem.2015.03.019

Su, J., Dai, M., He, B., Wang, L., Gan, J., Guo, X., et al. (2017). Tracing the origin of the oxygen-consuming organic matter in the hypoxic zone in a large eutrophic estuary: the lower reach of the Pearl River Estuary, China. *Biogeosciences* 14, 4085–4099. doi: 10.5194/bg-14-4085-2017

Tan, E., Wang, G., Moore, W. S., Li, Q., and Dai, M. (2018). Shelf-scale submarine groundwater discharge in the northern South China Sea and East China Sea and its geochemical impacts. *J. Geophys. Res. Oceans* 123, 2997–3013. doi: 10.1029/2017jc013405

Wang, X., Li, H., Jiao, J. J., Barry, D. A., Li, L., Luo, X., et al. (2015). Submarine fresh groundwater discharge into Laizhou Bay comparable to the Yellow River flux. *Sci. Rep.* 5:8814. doi: 10.1038/srep08814

Wang, X., Li, H., Zhang, Y., Zheng, C., and Gao, M. (2020). Investigation of submarine groundwater discharge and associated nutrient inputs into Laizhou Bay (China) using radium quartet. *Mar. Pollut. Bull.* 157:111359. doi: 10.1016/j.marpolbul.2020.111359

Wang, X., Li, H., Zheng, C., Yang, J., Zhang, Y., Zhang, M., et al. (2018). Submarine groundwater discharge as an important nutrient source influencing nutrient structure in coastal water of Daya Bay, China. *Geochim. Cosmochim. Acta* 225, 52–65. doi: 10.1016/j.gca.2018.01.029

Wang, X., Zhang, Y., Luo, M., Xiao, K., Wang, Q., Tian, Y., et al. (2021). Radium and nitrogen isotopes tracing fluxes and sources of submarine groundwater discharge driven nitrate in an urbanized coastal area. *Sci. Total Environ.* 763:144616. doi: 10.1016/j.scitotenv.2020.144616

Waska, H., Greskowiak, J., Ahrens, J., Beck, M., Ahmerkamp, S., Böning, P., et al. (2019). Spatial and temporal patterns of pore water chemistry in the inter-tidal zone of a high energy beach. *Front. Mar. Sci.* 6:154.

Waska, H., Simon, H., Ahmerkamp, S., Greskowiak, J., Ahrens, J., Seibert, S. L., et al. (2021). Molecular traits of dissolved organic matter in the subterranean estuary of a high-energy beach: indications of sources and sinks. *Front. Mar. Sci.* 8:607083.

Wu, K., Dai, M., Li, X., Meng, F., Chen, J., and Lin, J. (2017). Dynamics and production of dissolved organic carbon in a large continental shelf system under the influence of both river plume and coastal upwelling. *Limnol. Oceanogr.* 62, 973–988.

Wu, Z. J., Zhu, H. N., Tang, D. H., Wang, Y. Q., Zidan, A., and Cui, Z. G. (2021). Submarine groundwater discharge as a significant export of dissolved inorganic carbon from a mangrove tidal creek to Qinglan Bay (Hainan Island, China). *Continent. Shelf Res.* 223:11.

Xiao, K., Wilson, A. M., Li, H., Santos, I. R., Tamborski, J., Smith, E., et al. (2020). Large CO_2 release and tidal flushing in salt marsh crab burrows reduce the potential for blue carbon sequestration. *Limnol. Oceanogr.* 66, 14–29. doi: 10.1002/lno.11582

Xuan, Y., Tang, C., and Cao, Y. (2020). Mechanisms of nitrate accumulation in highly urbanized rivers: Evidence from multi-isotopes in the Pearl River Delta, China. *J. Hydrol.* 587:124924.

Ye, Y. X., Liang, B., Li, S. Y., and Hu, J. T. (2021). A study on the response of carbon cycle system in the Pearl River Estuary to riverine input variations. *J. Mar. Syst.* 215:14. doi: 10.1016/j.jmarsys.2020.103498

Yu, L. Q., Gan, J. P., Dai, M. H., Hui, C. R., Lu, Z. M., and Li, D. (2021). Modeling the role of riverine organic matter in hypoxia formation within the coastal transition zone off the Pearl River Estuary. *Limnol. Oceanogr.* 66, 452–468. doi: 10.1002/lno.11616

Zhang, L., Qin, X., Yang, H., Huang, Q., and Liu, P. (2013). Transported fluxes of the riverine carbon and seasonal variation in pearl river basin. *Environ. Sci.* 34, 3025–3034. (in Chinese with English abstract).

Zhang, Y., Li, H., Wang, X., Zheng, C., Wang, C., Xiao, K., et al. (2016). Estimation of submarine groundwater discharge and associated nutrient fluxes in eastern Laizhou Bay, China using Rn-222. *J. Hydrol.* 533, 103–113. doi: 10.1016/j.jhydrol.2015.11.027

Zhang, Y., Santos, I. R., Li, H., Wang, Q., Xiao, K., Guo, H., et al. (2020). Submarine groundwater discharge drives coastal water quality and nutrient budgets at small and large scales. *Geochim. Cosmochim. Acta* 290, 201–215. doi: 10.1016/j.gca.2020.08.026